25th Anniversary Article: Double Emulsion Templated Solid Microcapsules: Mechanics And Controlled Release

*Sujit S. Datta, Alireza Abbaspourrad, Esther Amstad, Jing Fan, Shin-Hyun Kim, Mark Romanowsky, Ho Cheung Shum, Bingjie Sun, Andrew S. Utada, Maike Windbergs, Shaobing Zhou, and David A. Weitz**

We describe how droplet microfluidics can be used to fabricate solid-shelled microcapsules having precisely controlled release behavior. Glass capillary devices enable the production of monodisperse double emulsion drops, which can then be used as templates for microcapsule formation. The exquisite control afforded by microfluidics can be used to tune the compositions and geometrical characteristics of the microcapsules with exceptional precision. We review the use of this approach to fabricate microcapsules that only release their contents when exposed to a specific stimulus – such as a change in temperature, exposure to light, a change in the chemical environment, or an external stress – only after a prescribed time delay, and at a prescribed rate.

1. Introduction

A microcapsule is a micrometer-scale particle, bubble, or liquid drop that is surrounded by a shell. This shell acts as a barrier separating the core from the outer environment. Microcapsules are thus attractive candidates for encapsulating, transporting, or controllably releasing a wide variety of technologically important active materials. These include surfactants for enhanced oil recovery,[1] agricultural chemicals,[2–8] food additives,[9–12] pharmaceuticals,[13–22] cosmetic components,[22–27] cells,[28–33] biochemical sensors,[34–37] catalysts for chemical reactions,[38,39] restorative agents for self-healing materials,[40,41] inks for carbonless copy paper,[42] or electronic inks.[43–45] In many of these applications, the microcapsule core is a liquid, and the shell is a solid that can resist a shear stress – this configuration enhances the robustness of the encapsulation. We focus on this important class of microcapsules here. Such microcapsules can be fabricated using a variety of techniques, including spray drying,[46–48] electrospraying,[49–51] coextrusion,[52–54] interfacial polymerization,[55–57] polymer phase separation,[58,59] layer-by-layer deposition,[60–62] or membrane emulsification.[63,64] However, these approaches typically yield microcapsules with polydisperse sizes and structures, highly variable loading levels, and poorly controlled release kinetics – even within the same batch; this can severely limit the use of microcapsules in many practical applications. It also precludes accurate characterization of the microcapsule physical properties. Many applications of microcapsules require their shells to have specific mechanical properties; understanding how exactly these properties depend on the structure and the composition of the shell can help guide the microcapsule fabrication process. However, because the fabrication of microcapsules with well-defined structures and compositions is challenging, systematic experiments to elucidate their mechanical response remain lacking.

Microfluidic technologies offer exquisite control over the flows of multiple fluids, and therefore, a way to overcome these limitations. One particularly promising route is the use of microfluidics to produce double emulsions, drops of the core material within drops of another fluid, which are themselves suspended in a continuous fluid phase. Subsequently solidifying the middle phase yields solid-shelled microcapsules. The interfacial tensions between the different fluids force the drops to be spherical; moreover, the drop sizes are determined by the shear forces exerted on the flowing fluids, which can be carefully tuned in a microfluidic device. As a result, double emulsion drops generated in microfluidics, and the microcapsules made from them, can be highly monodisperse, with compositions and morphologies that can be manipulated with a remarkable degree of accuracy.

In this review, we highlight recent developments in fabricating and characterizing solid-shelled microcapsules formed from microfluidically-generated double emulsion templates. We describe how, by precisely controlling the double emulsion composition and geometry, we fabricate microcapsules that only release their encapsulated contents when exposed to a specific stimulus – such as a temperature change, exposure to light, a change in the chemical environment, or an external stress – only after a prescribed time delay, and at a prescribed rate. This approach thus enables the design of microcapsules with release behavior tailored for specific applications.

Dr. S. S. Datta, Dr. A. Abbaspourrad, Dr. E. Amstad, Dr. J. Fan, Prof. S.-H. Kim, Dr. M. Romanowsky, Prof. H. C. Shum, Dr. B. Sun, Dr. A. S. Utada, Dr. M. Windbergs, Prof. S. Zhou, Prof. D. A. Weitz
Department of Physics and SEAS,
Harvard University
Cambridge, MA 02138, USA
E-mail: weitz@seas.harvard.edu

DOI: 10.1002/adma.201305119

2. Double Emulsion Templated Fabrication Of Solid-Shelled Microcapsules

A flowing thread of fluid breaks up into a series of monodisperse drops, due to the surface tension of the fluid; this configuration minimizes the fluid surface area, and hence, the surface energy. We exploit this Rayleigh-Plateau instability, using a glass capillary microfluidic device, to produce water-in-oil-in-water (W/O/W) double emulsion templates for microcapsules.[65] The inner aqueous phase contains the active material to be encapsulated; it may also contain a surface-active agent, such as poly(vinyl alcohol) (PVA), to prevent the liquid interfaces from coalescing, and a thickener, such as poly(ethylene glycol) (PEG), to enhance the viscosity of the solution. The middle oil phase is either a suspension of the shell material dispersed in a hydrophobic solvent, or a liquid form of the shell material itself. The outer phase is an aqueous solution containing a surfactant, such as PVA; after the microcapsules are fabricated, this outer fluid can be replaced or even removed.

A typical device consists of two tapered cylindrical capillaries inserted into the opposite ends of a square capillary, whose inner dimension is slightly larger than the outer diameter of the cylindrical capillaries; a schematic is shown in **Figure 1**(a). This arrangement aligns the cylindrical capillaries coaxially. We inject the inner aqueous phase through the left cylindrical capillary. To embed a drop of this phase within another fluid drop, we inject the middle oil phase, also from the left, through the interstitial space formed between the square and the cylindrical injection capillaries. This forms a coaxial flow at the tip of the tapered injection capillary. We inject the outer phase in the opposite direction, from the right, through the interstitial space formed between the square and the right cylindrical capillaries; the three fluids thus become hydrodynamically focused and flow through the orifice of the right cylindrical capillary. We operate this microfluidic device in the dripping regime, in which the inner and middle phases break up after entering the right capillary, forming monodisperse W/O/W double emulsion drops. The double emulsions formed using this approach have average outer radii, R_0, on the order of tens to hundreds of microns. This value can be controlled by the size of the orifice, as well as the flow rates of the inner, middle, and outer phases, Q_i, Q_m, and Q_o, respectively;[65] it increases with Q_i and Q_m, while it decreases with Q_o, as exemplified by the data shown in **Figure 2**(a). The double emulsion middle phase thickness can also be controlled by the flow rates used;[66] it increases with Q_m, while it decreases with Q_i and Q_o, as shown by the data in Figure 2(b).

Due to the difference in density between the inner and middle phases, after these drops are collected, they become increasingly inhomogeneous, with a spatially-varying middle phase thickness. For example, if the inner phase is lighter than the middle phase, the inner drop will rise; this causes the middle phase to gradually thin on the top side of each double emulsion drop. Eventually, the middle phase can become so thin that it ruptures, precluding the use of the double emulsion as a template for microcapsule fabrication. This thinning process can be quantified using a lubrication analysis of the flow in the middle phase:[67] balancing gravity with the viscous drag on the inner drop yields a characteristic time scale for the

Sujit S. Datta obtained his PhD in Physics at Harvard University in 2013, in the group of Prof. David Weitz. He grew up in Toronto, Canada, and graduated from the University of Pennsylvania with a BA in Physics and Mathematics and a MS in Physics. His PhD research focused on understanding the physics of flow through porous materials, as well as the mechanics and release properties of microcapsules.

Alireza Abbaspourrad is a postdoctoral researcher in the Weitz lab at Harvard University. He received his MSc in Chemistry from Ferdowsi University in 2000 and his PhD in Organic Chemistry from the Isfahan University of Technology in 2006, under the supervision of Prof. Mehran Ghiaci. He then worked as a postdoctoral researcher with Prof. Stanislav Moshkalev at the University of Campinas in Brazil, working on the development of novel carbon nanotube gas sensors. His current research interests are in soft-matter physics, microfluidics, and single-cell analysis using droplet-based microfluidics.

David A. Weitz is the Mallinckrodt Professor of Physics and Applied Physics at Harvard University, where he has appointment in both the Physics Department and the School of Engineering and Applied Sciences. He received his PhD in Physics from Harvard, and then worked at Exxon Research and Engineering for nearly 18 years. He then was a professor of Physics at the University of Pennsylvania before joining to Harvard, where he leads the experimental soft condensed matter physics research group. His research efforts include soft matter physics, biophysics and biotechnology. He is Director of Harvard's NSF-funded Materials Research Science and Engineering Center, and co-Director of the BASF Advanced Research Initiative and the Kavli Institute of Bionano Science and Technology. He is a member of the National Academies of Science and the American Academy of Arts and Science.

Adv. Mater. **2014**,
DOI: 10.1002/adma.201305119

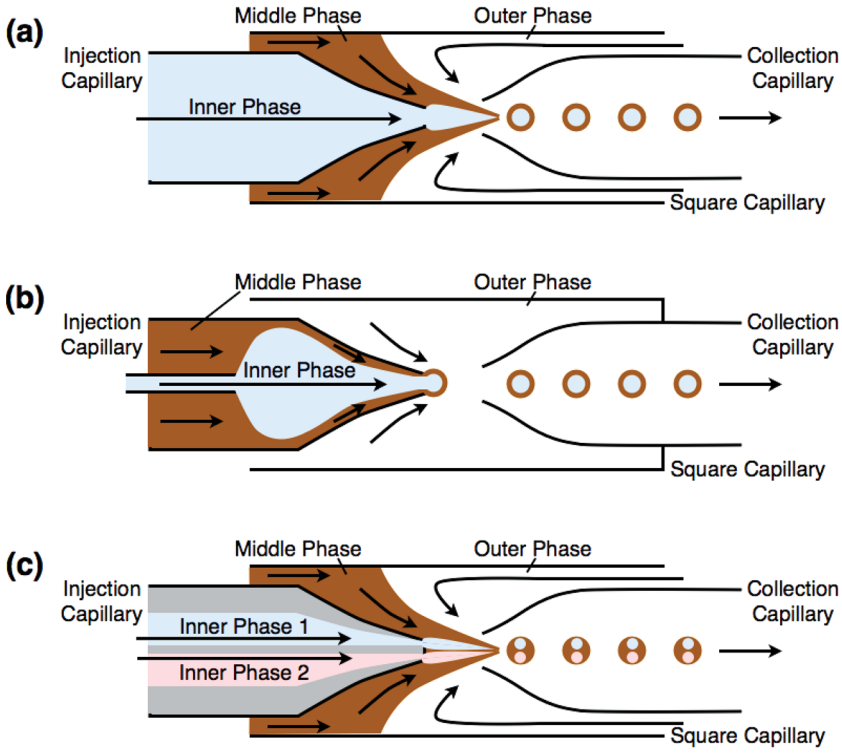

Figure 1. Schematic showing the microfluidic production of double emulsion templates with (a) thick middle phases,[65] (b) ultra-thin middle phases,[69] and (c) multiple inner drops.[70] After the templates are produced, we use the middle phase to form solid shells, thus yielding monodisperse microcapsules.

middle phase to thin completely, $9\mu_m(R_0 - h_0)/2\Delta\rho g h_0^2$, where μ_m is the viscosity of the middle phase, $\Delta\rho$ is the difference in the densities of the middle and inner phases, g is gravitational acceleration, and h_0 is the average middle phase thickness. Tuning experimental conditions to increase this time scale – for example, by increasing μ_m or decreasing $\Delta\rho$ – thus provides a route towards enhancing the uniformity of the microcapsule shell. This time scale increases particularly precipitously as h_0 decreases: the increased confinement provided by a thinner middle phase increases the viscous resistance to the motion of the inner drop.[68] Consequently, double emulsions with thinner middle phases remain stable over a longer time period; it is thus highly desirable to form double emulsion templates with ultra-thin middle phases.

However, forming ultra-thin middle phases, with thicknesses below the micron scale, is challenging; it requires extremely low values of Q_m, which can be difficult to achieve, due to the inevitable fluctuations in the flow that arise in the operation of a syringe pump. To overcome this limitation, we use a different microfluidic approach to generate double emulsion drops with ultra-thin middle phases.[69] We again use two tapered cylindrical capillaries inserted into the opposite ends of a square capillary. Unlike the previous case, however, we inject the middle oil phase through the left cylindrical capillary; moreover, we insert yet another smaller capillary into this capillary, and use the smaller capillary to simultaneously inject the inner aqueous phase, as schematized in Figure 1(b). We treat the inner wall of the left injection capillary with n-octadecyl trimethoxy silane; this renders its inner surface hydrophobic, preventing wetting of the aqueous phase. Under these conditions, the inner aqueous phase forms large water-in-oil emulsion drops within the injection capillary. We then flow the outer aqueous phase, also from the left, through the interstitial space formed between the square and the cylindrical injection capillaries. The three fluids flow into the orifice of the right tapered capillary; we coat this with 2-[methoxy(polyethyleneoxy)propyl] trimethoxy silane to render its surface hydrophilic, preventing wetting of the middle oil phase on the capillary wall. We operate

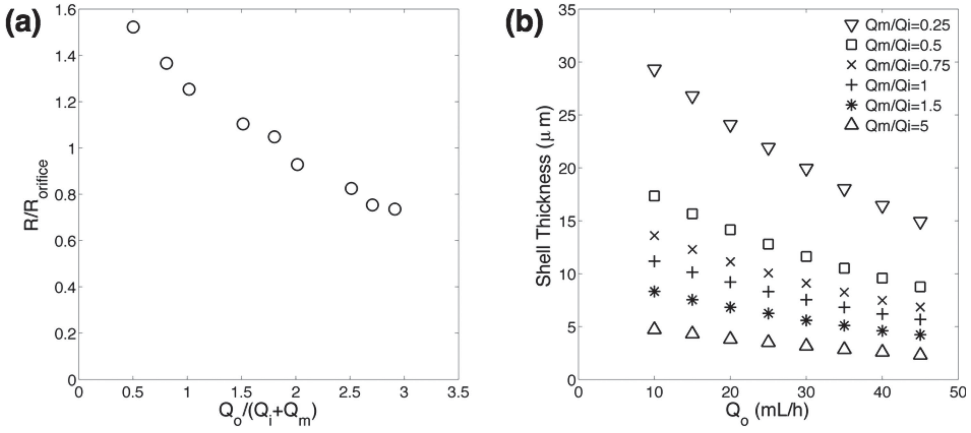

Figure 2. Dependence of the double emulsion template (a) radius, R, and (b) middle phase thickness, on the flow rates used. $R_{orifice}$ is the radius of the capillary orifice, while Q_i, Q_m, and Q_o are the flow rates of the inner, middle, and outer phases, respectively. Data in (a) and (b) are reproduced with permission from Ref. [65] and Ref. [66], respectively. Copyright 2005, American Association for the Advancement of Science and Copyright 2012, Springer. The sum of the middle and inner fluid flow rate is 1 mL h^{-1} in (a) and 5 mL h^{-1} in (b).

this microfluidic device in the dripping regime, in which the water drops become re-emulsified at the tip of the right tapered capillary. This process forms monodisperse W/O/W double emulsion drops with middle phase thicknesses as small as tens of nanometers.

In some applications, multiple, incompatible active materials must be encapsulated within the same microcapsule. This requires microcapsules containing multiple core compartments. Our microfluidic approach provides a straightforward way to fabricate templates for such microcapsules in one single step: instead of injecting just one inner phase through a single-bore tapered cylindrical capillary, we inject two, three, or four different inner phases, each one through a different bore of a dual, triple, or quadruple-bore injection capillary, respectively.[70] Similar to the case of a single-bore capillary, the different injected fluid streams are encased by the middle oil phase, and break up after entering the right capillary, as schematized in Figure 1(c). This process forms multiple inner drops, each containing a different active, within each double emulsion drop.

After the double emulsion templates are produced, we use their middle phase to form solid shells. Two possible approaches to fabricating this shell are polymerization and solvent evaporation. In the first approach, the middle phase is a monomer solution containing a crosslinker; when polymerized, this solution forms a solid shell composed of cross-linked polymers. Solidification thus occurs either after sufficient time has elapsed for the polymerization to occur, or can be triggered at a specific time by the inclusion of stimulus-responsive molecular initiators. For example, including a photoinitiator enables the middle phase to be rapidly polymerized, forming a solid shell, simply by exposure to UV light.[71] In the second approach, the middle phase is a dispersion of the shell material, such as a polymer or colloidal particles, in a volatile solvent; as this solvent evaporates, the shell material precipitates. The middle phase solvent either evaporates completely, or, if it is a mixture of different solvents, it can dewet from the surface of the inner drop, ultimately yielding a solid shell.[72] In both approaches to shell formation, the structure of the resultant microcapsule depends sensitively on the composition and the geometrical characteristics of the double emulsion template used.

3. Mechanics Of Solid-Shelled Microcapsules

Because their structures and compositions can be precisely controlled, microcapsules produced from microfluidically-generated templates provide a useful experimental system to elucidate key physical properties, such as the microcapsule mechanical stability. One common way of characterizing the mechanical properties of the thin, spherical shell of a microcapsule is to investigate its response to a uniform externally imposed pressure. If this pressure is sufficiently small, a homogeneous shell of uniform thickness supports a compressive stress, and it shrinks uniformly. Above a threshold pressure, however, the strain energy required to shrink the shell becomes larger than the energy required to form a localized, circular indentation in its surface; consequently, the shell buckles. Balancing these two energies yields a threshold buckling pressure, $\Pi^* = \frac{2E}{\sqrt{3(1-\nu^2)}}\left(\frac{h_o}{R_o}\right)^2$, where h_0 and R_0 are the shell thickness and outer radius, respectively, and E and ν are the Young's modulus and Poisson's ratio of the shell material, respectively.[73] One way of imposing the external pressure by dissolving a non-adsorbing osmolyte in the outer fluid surrounding the microcapsules; the resultant osmotic pressure, Π, can then be estimated using the van't Hoff relationship, $\Pi = cN_ak_BT$, where c is the osmolyte concentration, N_a is Avogadro's constant, k_B is Boltzmann's constant, and T is temperature.[74] Another way is to simply dry a microcapsule suspension; as the outer fluid evaporates, tiny menisci form in the pores of the microcapsule shells. This results in a capillary pressure difference across each shell; the pressure outside the shell is larger by $P_c \approx 2\gamma/a_p$, where γ is the surface tension of the outer fluid in air and a_p is the characteristic pore radius.[75,76] For both of these cases, experiments on homogeneous microcapsules of varying h_0 confirm the validity of the predicted threshold.[74–76]

In many cases, however, microcapsules have inhomogeneous shells, characterized by spatially varying thicknesses and elastic constants; these variations can arise during the microcapsule fabrication process. For example, as described in Section 2, if the inner phase of the double emulsion templates used to fabricate microcapsules is less dense than the middle phase, the inner drop will gradually rise. We use this effect to prepare microcapsules with spatially varying shell thicknesses $h(\theta) = h_0 - \delta\cos\theta$, where θ is measured from the top of each microcapsule and δ is the total distance moved by the inner drop;[67] this geometry is schematized in **Figure 3**(a). Polymerizing the capsules using UV light, either as the double emulsions are produced in situ, or after waiting a time t_w after collecting them, produces separate batches of microcapsules characterized by varying degrees of shell inhomogeneity.

Because the stretching and bending stiffnesses of the shell scale as ~h and ~h^3, respectively, the thinnest part of the microcapsule shell should be the weakest,[77] as confirmed by the micrographs in Figure 3(b). We thus expect the onset of buckling to be determined by the deformations in this part of the shell. Applying shell theory to this inhomogeneous geometry yields a modified prediction of the threshold buckling pressure, $\Pi^* = \frac{2E}{\sqrt{3(1-\nu^2)}}\left(\frac{h_o-\delta}{R_o}\right)^2$;[67] consistent with our expectation, this threshold is the same as the threshold for a homogeneous shell, but with the shell thickness replaced by the thickness of the thinnest part of the shell, h_0-δ. Experiments performed on microcapsules of varying h_0, over a broad range of pressures, confirm this prediction, as shown in Figure 3(c-d).[67] These results indicate that the onset of microcapsule buckling is well described by shell theory, even for highly inhomogeneous microcapsules.

Interestingly, even above this threshold pressure, the microcapsules do not buckle immediately; the time delay before the onset of buckling, τ, strongly decreases with osmotic pressure. This behavior likely reflects the dynamics of fluid flow through the microcapsule shell; within this picture, for a microcapsule to buckle, it must eject a volume ΔV^* from its interior. The time delay can then be estimated as $\tau = \Delta V^*/Q$, where both

Adv. Mater. 2014,
DOI: 10.1002/adma.201305119

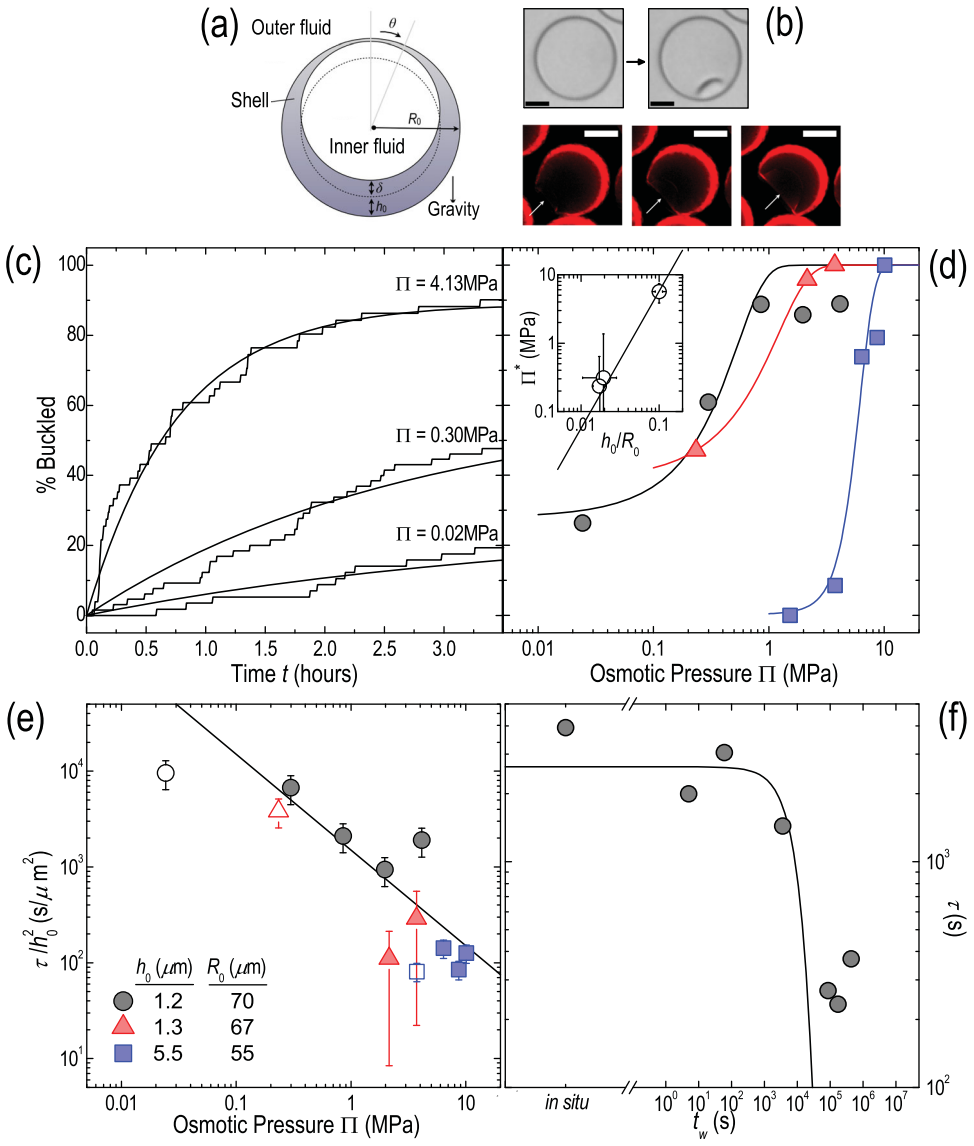

Figure 3. (a) Schematic showing the geometry of inhomogeneous double emulsion-templated microcapsules. (b) Optical and fluorescence micrographs show that buckling begins at the thinnest part of the microcapsule shell. Scale bars denote 50 μm. (c) Fraction of capsules buckled over time, for three different osmotic pressures Π, for capsules with $\delta/h_0 = 0.20$. Smooth lines show exponential fits. (d) Total fraction of capsules that ultimately buckle over time for varying Π, for capsules with h_0, R_0, and $\delta/h_0 = 1.2$ μm, 70 μm, and 0.20 (circles), 1.3 μm, 67 μm, and 0.23 (triangles), and 5.5 μm, 55 μm, and 0.19 (squares), respectively. Smooth curves are fits to the data using the cumulative distribution function of the normal distribution. Inset shows mean osmotic pressure of each fit versus h_0/R_0; vertical and horizontal error bars show standard deviation of each fit and estimated variation in h_0/R_0, respectively. Straight line shows predicted $(h_0/R_0)^2$ scaling. (e) Time delay before the onset of buckling, τ, normalized by h_0^2, for varying Π, for the same capsules as in (d). Filled points show $\Pi > \Pi^*$ while open points show $\Pi < \Pi^*$. Vertical error bars show uncertainty arising from estimated variation in h_0. Black line shows predicted Π^{-1} scaling. (f) Time delay τ decreases with the wait time before a shell is polymerized, t_w. Black line shows theoretical prediction coupling shell theory and Darcy's law. Reproduced with permission.[67] Copyright 2012, American Physical Society.

δV^* and Q, the volumetric rate of fluid ejection from the interior, depend on δ/h_0. Calculating δV^* using shell theory, and Q using Darcy's law for flow through a permeable material, thus yields an estimate for the time delay before buckling, $\tau \approx \frac{V_0}{Q_0}\sqrt{\frac{3(1-\nu)}{1+\nu}}\frac{h_o}{R_o}\left(1-\frac{\delta}{h_o}\right)^2$, where V_0 is the initial microcapsule volume, $Q_0 \equiv 4\pi R_0^2 \Pi k/\mu h_0$, μ is the fluid viscosity, and k is the shell permeability. Experiments on microcapsules of varying inhomogeneities, performed over a broad range of osmotic pressures, directly confirm this prediction, as shown in Figure 3(e-f).[67] These results suggest that the dynamics of microcapsule buckling can be understood by combining shell theory with Darcy's law for flow through the microcapsule shell, even for very inhomogeneous shells.

Because buckling is determined by the deformations at the thinnest part of the microcapsule shell, the location of this "weak spot" can be used to guide where buckling occurs. For example, forming double emulsions with multiple inner drops, each of radius greater than half the radius of the outer drop,

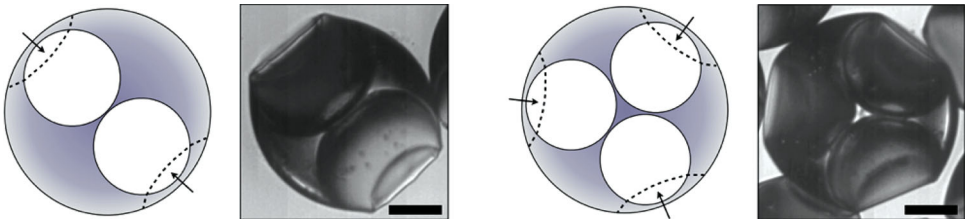

Figure 4. Microcapsules with two or three spherical interior compartments buckle at "weak spots" (arrows). This forms shapes with two or three equally-spaced circular indentations after buckling (micrographs). Scale bars denote 100 μm. Reproduced with permission.[67] Copyright 2012, American Physical Society.

forces the inner drops to pack closely. Polymerizing these double emulsions thus forms solid-shelled microcapsules having multiple equally-spaced "weak spots" in their shells, as schematized in **Figure 4**. Subjecting these microcapsules to a large osmotic pressure forces them to buckle; unlike the case of a microcapsule with a single core, however, these microcapsules buckle through the formation of multiple, localized, equally-spaced indentations at the "weak spots".[67] Two examples are shown in Figure 4. This approach is thus a versatile means of creating microcapsules of desired symmetries; these can, for example, be used to guide colloidal self-assembly through lock-and-key binding of colloidal particles to the indentations formed during buckling.[78]

4. Controlled Release From Solid-Shelled Microcapsules

4.1. Release Triggered by a Change in Temperature

Many applications of microcapsules require them to stably encapsulate their contents, releasing them only after exposure to a specific stimulus. Double emulsion templates provide a versatile means to fabricate such microcapsules – for example, by using shell materials that physically change in response to the stimulus, triggering release in the process. An important class of stimuli is a change in temperature; this finds applications in transporting and releasing food additives, cosmetics, or drugs, which often require release to be triggered at body temperature (37 °C). Lipids or hydrocarbons are a natural choice of the shell material in this case: many of them are solid at room temperature, enabling robust encapsulation under ambient conditions, but melt at temperatures in the range 32–44 °C, releasing the encapsulated active when heated. To fabricate microcapsules using these materials, we use a microfluidic device, heated well above the melting point of the shell material, T_m, to form double emulsion templates. After the double emulsions are formed, they are collected in a cooled vial to speed solidification of their shells. We have used this approach to form microcapsules with shells composed of glycerides (T_m = 33–35 °C), nonadecane (T_m = 32 °C), icosane (T_m = 37 °C), paraffin oil (T_m = 42–44 °C), and biodegradable, food-grade lipids (T_m = 33.5–35.5 °C);[79,80] an example is shown in **Figure 5**.

These microcapsules can be used to encapsulate and release a wide variety of active materials, including microparticles, polysaccharides, positively- and negatively-charged dyes, hydrophilic drugs, and even surfactants. Moreover, this double emulsion-templated approach can be used to encapsulate and release multiple, incompatible actives. One way to do this is to use a multi-bore injection tube to form double emulsions containing multiple inner drops, each containing a separate active. Another way is to dissolve the different actives in the inner and middle phases of the double emulsion; this approach requires the actives to dissolve preferentially in the different phases, which is frequently the case. As an application of this concept, we use two anticancer drugs which are known to act synergistically; their performance is thus greatly enhanced if they are released simultaneously after being administered to a patient. The first, doxorubicin hydrochloride, is hydrophilic, and is dissolved in the aqueous inner double emulsion drop, while the second, paclitaxel, is hydrophobic, and is dissolved in the double emulsion middle phase while it is still molten. Cooling the double emulsions forms microcapsules containing the hydrophilic drug in their cores and the hydrophobic drug in their solid shells.[80] These microcapsules can then be administered to a patient as a liquid suspension, or can be filtered and dried, forming a free-flowing powder, which can then be packed into solid particles. Importantly, the lipid shell melts at 33.5–35.5 °C; thus, under these conditions, the microcapsules in the particles release both drugs simultaneously, as shown by the micrographs in **Figure 6**. The efficacy of this approach is demonstrated by incubating the drug-containing particles with two different lines of cancer cells: all of the cells in both cell lines die after 20 hours of incubation with the particles.

Another approach to fabricating microcapsules with temperature-controlled release is to use thermosensitive polymers to form the shells. One commonly-used polymer is

Figure 5. Microcapsule with a paraffin shell, encapsulating toluidine blue, releases its contents when heated. At 45 °C, the shell becomes a liquid (second frame), enabling the inner core to coalesce with the outermost phase (third frame). After five minutes of heating, the encapsulated dye is almost entirely released (fourth frame). Figure is reprinted with permission from Ref. [79]; Copyright 2010, American Chemical Society.

Adv. Mater. **2014**,
DOI: 10.1002/adma.201305119

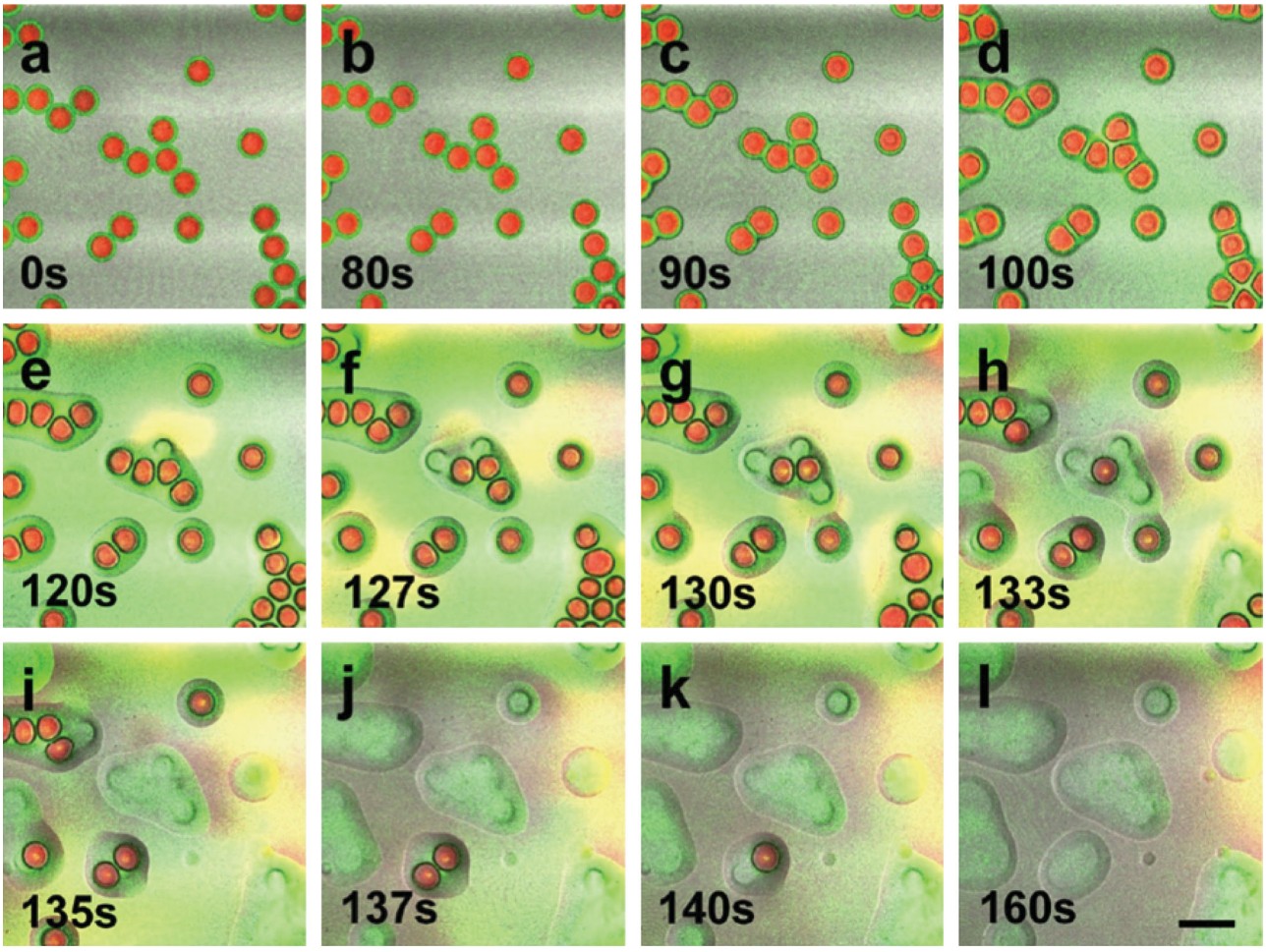

Figure 6. Fluorescence micrographs showing release from microcapsules with lipid shells at 37 °C; while these shells are solid at room temperature, they melt at 33.5–35.5 °C. A hydrophilic drug, doxorubicin, is fluorescently labeled in red, and is initially encapsulated in the microcapsule core, while a hydrophobic drug, paclitaxel, is fluorescently labeled in green, and is initially embedded in the microcapsule shell. Upon heating, both drugs are released simultaneously in a matter of minutes. Scale bar denotes 200 μm. Reproduced with permission.[80] Copyright 2013, American Chemical Society.

poly[N-isopropylacrylamide] (pNIPAm); when cross-linked, this polymer forms a solid hydrogel under ambient conditions. At temperatures higher than the lower critical solution temperature, 32 °C, the hydrogen bonds between the hydrophilic amine chains become disrupted; consequently, the polymer undergoes a reversible phase transition to a shrunken dehydrated state.[81] This shrinkage introduces defects into the microcapsule shell, enabling the encapsulated active to be released. This approach can also be used to trigger release from polymerosomes, microcapsules whose shells are composed of bilayers of amphiphilic block copolymers.

We form the polymerosomes using dewetting from W/O/W double emulsion templates.[82] The middle oil phase contains a mixture of PEG-b-poly[lactic acid] (PEG-b-PLA) and thermosensitive pNIPAm-b-poly[lactic-co-glycolic acid] (pNIPAm-b-PLGA) diblock copolymers; this mixture forms a solid shell when the solvent in the middle phase is removed. Similar to the case of a pNIPAm shell, the shrinkage of the pNIPAm-b-PLGA introduces defects into the polymerosome shell, enabling the encapsulated material to be released, as shown in **Figure 7**. Moreover, the release can also be triggered by stimuli other than a change in the external temperature. For example, we incorporate hydrophobized metallic nanoparticles into the double emulsion middle phase; this embeds them into the polymerosome shell during the solvent removal. The nanoparticles heat up when illuminated with a laser, collapsing the pNIPAm block of the pNIPAm-b-PLGA shell; this again introduces defects into the polymerosome shell, and the encapsulated contents are released.

A change in temperature can also be used to trigger release from colloidosomes, microcapsules comprised of a shell of densely-packed colloidal particles. A significant problem inherent to colloidosomes is that they are leaky, due to the large pores formed between the particles; if the encapsulated active is sufficiently small, it can diffuse through these pores and become spontaneously released. Controlling this release requires the permeability of the shell, which is determined by the morphology of the pores, to be precisely controlled. One approach to achieving this is to fabricate colloidosomes, with shells composed of close-packed β-cyclodextrin (β-CD) nanoparticles, using dewetting from W/O/W double emulsion templates; to render the colloidosomes thermosensitive, we dissolve a thermo-sensitive triblock copolymer, Pluronic L31,

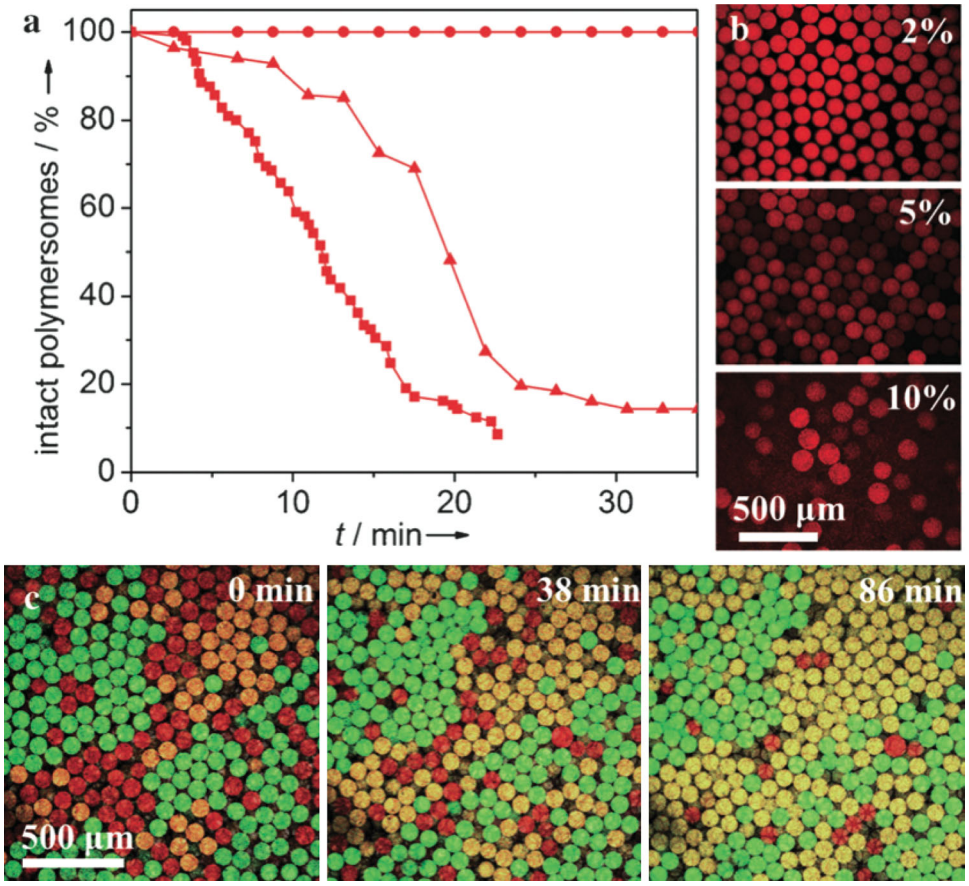

Figure 7. Double emulsion-templated polymerosomes exhibit thermosensitive release. (a) Fraction of intact polymerosomes decreases with incubation time at 40 °C; circles, triangles, and squares are for PEG-b-PLA polymerosome shells including 2 wt%, 5 wt%, and 10 wt% PNIPAM-b-PLGA, respectively. Confocal micrographs for these polymerosomes after 20 minutes of incubation are shown in (b). Confocal micrographs of a mixture of three different populations of polymerosomes, incubated at 40 °C, over time; polymerosomes with shells comprised of PEG-b-PLA, PEG-b-PLA with 5 wt% PNIPAM-b-PLGA, and PEG-b-PLA with gold nanoparticles are shown in green, red, and yellow, respectively. Only the polymerosomes with shells containing PNIPAM-b-PLGA release their contents. Reproduced with permission.[82] Copyright 2012, Wiley-VCH.

in the inner aqueous phase.[83] The uniformity and narrow size distribution of the double emulsion-templated colloidosomes ensures that their cores are uniformly loaded with the thermosensitive copolymer. Under ambient conditions, this polymer adsorbs to the surfaces of the β-CD nanoparticles, blocking the pores between them and fully encapsulating an active material inside the core, as schematized in the top panel of **Figure 8**. However, at sufficiently high temperatures, the polymer desorbs from the β-CD particle surfaces, forming aggregates that instead remain dispersed within the colloidosome cores, as schematized in the bottom panel of Figure 8. This opens the pores, enabling the encapsulated active to be released through them. This process is reversible, proceeding or becoming arrested on demand through a change in temperature.

4.2. Release Triggered by a Chemical Reaction

A second important class of stimuli for microcapsule release is a change in the external chemical environment; this can trigger a chemical reaction with the microcapsule shell. To address this need, we form solid-shelled microcapsules from double emulsion templates whose middle phase is a polymer dispersed in a volatile solvent; this solvent evaporates after drop formation, and the polymer precipitates, forming a solid shell. In some cases, the shell can begin to dissolve immediately after it is formed, due to its exposure to the external aqueous environment; for example, microcapsules made from PLA begin to degrade due to the hydrolysis of the ester groups in the polymer chain.[69] Micrographs showing release from these microcapsules are shown in **Figure 9**. In other cases, we use responsive polymers that dissolve only after exposure to a desired chemical stimulus, which forces the microcapsule shell to degrade and ultimately release its contents. One key example of such a stimulus is exposure to a hydrocarbon oil; this is particularly important in enhanced oil recovery applications in which a surfactant must be transported to and released at oil surfaces. To fabricate microcapsules that respond to this stimulus, we use polystyrene (PS), a polymer that absorbs oil, undergoing a solid-to-liquid phase change in the process.[84] Thus, when a microcapsule with a PS shell approaches a hydrocarbon oil surface, the shell liquefies. The localized defect thus formed in the shell permits the encapsulated active to be ejected from the microcapsule core, toward the surface of the oil, as shown in **Figure 10**.

Adv. Mater. **2014**,
DOI: 10.1002/adma.201305119

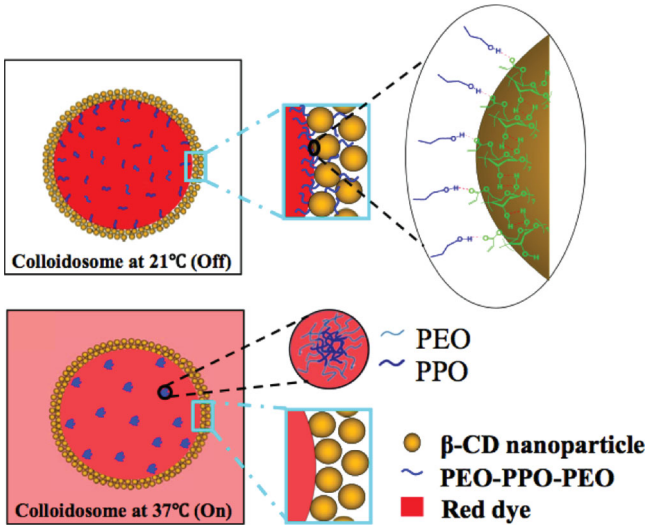

Figure 8. Schematic showing mechanism of thermosensitive release from double emulsion-templated nanoparticle colloidosomes. (a) Under ambient conditions, the PEO-PPO-PEO copolymers block the interstitial pores in the shell, switching off the release and enabling robust encapsulation of a dye in the core. (b) At 37 °C, the copolymers aggregate, opening the interstices and switching on the release from the colloidosome core. Reproduced with permission.[83] Copyright 2013, Wiley-VCH.

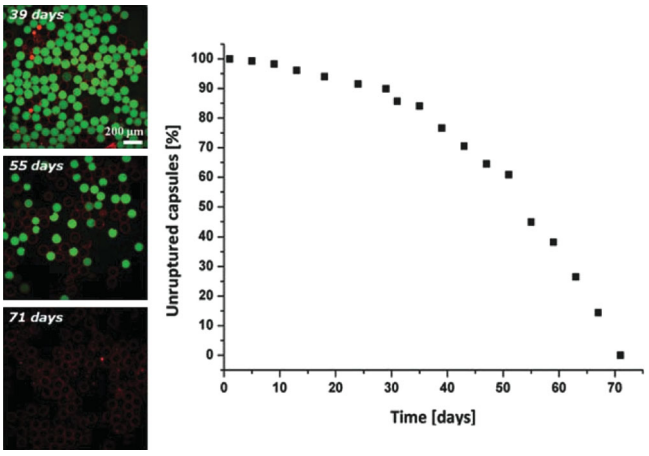

Figure 9. Double emulsion-templated microcapsules with ultra-thin PLA shells release their contents upon exposure to water. Confocal micrographs show examples of dyed microcapsules 39, 55, and 71 days after exposure. The capsules are all fully degraded, and the encapsulated material is completely released, after 70 days. Reproduced with permission.[69] Copyright 2011, Royal Society of Chemistry.

Another important trigger for release is pH; this may find particular use in biological applications. We thus form microcapsules with solid shells composed of pH-responsive biocompatible polymers.[85] When exposed to a trigger pH, the polymer chains making up the shells become highly charged, repel each other, and dissolve in the outer fluid;[86,87] consequently, the shells degrade, ultimately releasing their contents, as shown in **Figure 11**. The exact pH that triggers the release is set by the choice of the polymer: a base-sensitive polymer, such as an anionic diblock copolymer of methacrylic acid and methyl methacrylate (PAA-b-PMMA), dissolves at pH > 7, while an acid-sensitive polymer, such as a cationic triblock copolymer of poly-[(2-dimethylaminoethyl)-methacrylate-n-butyl methacrylate] (DMAEMA-MMA-BMA), dissolves at pH < 6. This experimental approach can thus be used to trigger release over a range of different pH conditions. To illustrate this, we mix two different populations of acid- and base-responsive microcapsules. The acid-responsive microcapsules encapsulate a yellow dye, as well as 1μm tracer particles, while the base-responsive microcapsules encapsulate a green dye. When the microcapsules are first exposed to an acidic pH of 5, the acid-responsive microcapsules degrade and quickly release their contents, as shown in the second and third frames of **Figure 12**; by contrast, the base-responsive microcapsules remain stable, and continue to encapsulate their contents. We then raise the pH of the outer fluid to 9; this forces the base-responsive microcapsules to also release their contents, as shown in the fourth and fifth frames of Figure 12. Thus, by fabricating different microcapsules using different pH-responsive polymers, we can program the sequential release of different actives. This approach could be applied, for example, in the delivery of pharmaceutical products to different areas of the human digestive system, which can be characterized by significantly different pH values.

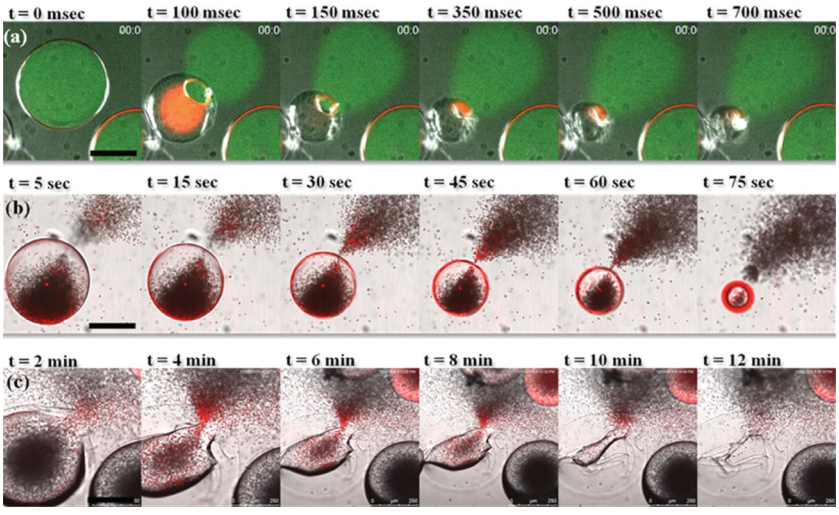

Figure 10. PS microcapsules release their contents when exposed to (a) pure toluene, (b) 50 wt% toluene in water, and (c) 10 wt% toluene in water. Reproduced with permission.[84] Copyright 2013, American Chemical Society.

This approach can also be used to design microcapsules whose release is triggered by common water contaminants, such as fluoride; for example, the microcapsules could then release chemical agents that aid in water remediation. Unfortunately, contaminants often present themselves only at minuscule – but still environmentally detrimental – concentrations; thus, the response of the polymer making up the microcapsule shell must be extremely sensitive. To address this need, we fabricate microcapsules with shells composed of poly[phthaldehyde] (PPHA).[88] Crucially,

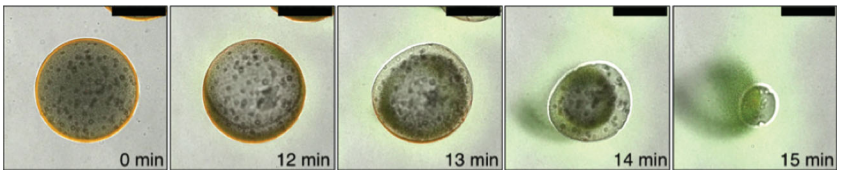

Figure 11. Optical micrographs, with fluorescence micrographs superimposed, showing the degradation of the base-responsive shell of a double emulsion-templated microcapsule, leading to the release of an encapsulated green dye. The microcapsules also encapsulate, and subsequently release, polystyrene tracer particles (grey). Scale bar denotes 100 μm. Time stamp shows time elapsed after pH is raised to 9. Reproduced with permission.[85] Copyright 2013, American Chemical Society.

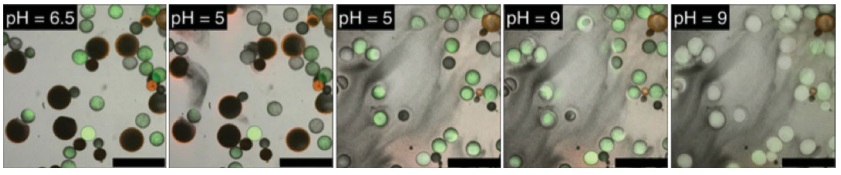

Figure 12. Optical micrographs, with fluorescence micrographs superimposed, showing the release of a yellow encapsulated dye only from acid-responsive double emulsion-templated microcapsules when the pH is reduced to 5 [second and third frames]. An encapsulated green dye, along with polystyrene tracer particles (grey), is then released from base-responsive PAA-b-PMMA microcapsules when the pH is increased to 9 [fourth and fifth frames]. Scale bar denotes 500 μm. Reproduced with permission.[85] Copyright 2013, American Chemical Society.

we functionalize each PPHA molecule with a fluoride-responsive end-cap; upon exposure to fluoride, the bond between the polymer and this end-cap is broken, forcing the entire molecule to depolymerize quickly. This unique behavior enhances the sensitivity of the microcapsule shell to fluoride; for example, upon exposure to just 50 mM aqueous fluoride, microcapsules with 1.8μm thick shells fully release their contents within three days, as shown in **Figure 13**. This approach may thus find use in the directed remediation of contaminated water supplies.

4.3. Controlling Release Kinetics

In the examples described in Section 4.2, the time at which the microcapsule contents are released depends sensitively on the shell thickness: microcapsules with thicker shells take longer to fully degrade and ultimately release their contents, as exemplified by the data shown in **Figure 14**.[66,85] By enabling the production of microcapsules with different shell thicknesses, the precise flow control afforded by microfluidics thus provides a straightforward way to control the time of release.

Many of the responsive polymers used to make microcapsules phase separate when solidified in the presence of another, non-responsive, polymer. We use this effect to prepare hybrid microcapsules that, when exposed to a chemical stimulus, selectively dissolve only at parts of their shells, as schematized in the top panel of **Figure 15**. This enables us to independently control the permeability of the shell, and thus, the rate of release. To demonstrate this concept, we prepare hybrid pH-responsive microcapsules using our microfluidic approach;[85] we use a mixture of the base-responsive polymer described in Section 4.2 with another, pH-unresponsive, ethylene glycol phenyl ether methacrylate monomer, also including a crosslinker and a photoinitiator. We irradiate the double emulsion drops with UV light as they are formed in the microfluidic device; this selectively photo-polymerizes the pH-unresponsive monomer. We then collect the double emulsion drops; as the middle phase solvent evaporates, the pH-responsive polymer precipitates, completing the formation of a solid, hybrid shell. When exposed to a stimulus pH, only the pH-responsive portions of this shell dissolves, forming holes through which the encapsulated active is released. The size of these holes, and thus, the permeability of the shell, depends sensitively on the shell composition: for example, shells comprised of a larger proportion of pH-unresponsive polymer develop smaller holes, and thus, the release of the encapsulated active is slower, as shown in Figure 15. This approach is thus a straightforward way to tune the microcapsule release rate.

4.4. Release Triggered by an External Stress

Another important class of stimuli for microcapsule release is an externally imposed stress. This idea is central to one of the earliest and most ubiquitous applications of microcapsules: to encapsulate and release the colorless ink used in carbonless copy paper. The microcapsules coat each sheet of paper, only releasing the encapsulated ink when pressed on sufficiently hard by a pen; the released ink then reacts with a developer coating the underlying sheet, forming a mark that reproduces the pen's trace.[42] We use a similar principle to trigger release from microcapsules in suspension. We use double emulsion templates to fabricate PS

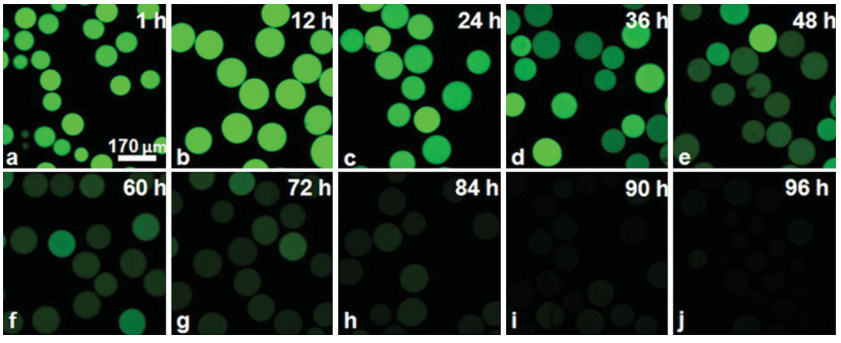

Figure 13. PPHA microcapsules release a fluorescent dye when exposed to 50 mM aqueous fluoride, as shown by the fluorescence micrographs in (a-j). Reproduced with permission.[88] Copyright 2013, American Chemical Society.

Adv. Mater. **2014**,
DOI: 10.1002/adma.201305119

or polystyrene-polyisoprene-polystyrene (PS-PIP-PS) microcapsules;[84] the former have brittle shells, which are more likely to rupture under an external stress, while the latter are more ductile, and are more likely to stably encapsulate an active material, even when deformed. To illustrate this difference in their response, we flow 110 μm diameter microcapsules of both types through a narrow constriction, 70 μm in diameter, formed in a 580 μm diameter glass capillary. The brittle PS microcapsules irreversibly rupture when they reach the constriction, due to the large stress imposed on their shells, and they release their contents, as shown in **Figure 16**(a). In stark contrast, the ductile PS-PIP-PS microcapsules squeeze through the constriction without rupturing, ultimately recovering their original spherical shape, as shown in Figure 16(b). In this application, as in numerous others, the utility of the microcapsules depends sensitively on the mechanical properties of their shells.

5. Conclusion

We have described the straightforward fabrication of solid-shelled microcapsules using double emulsion templates produced in microfluidics. This approach yields an unprecedented level of control over the microcapsule size, composition, and geometrical structure. This enables us to fabricate microcapsules that robustly encapsulate an active material, releasing it only when exposed to a desired stimulus, such as a change in temperature, exposure to light, a change in the chemical environment, or an external stress; moreover, we can tune exactly when the encapsulated active is released, and at what rate. Such microcapsules are thus useful for a variety of applications ranging from fundamental studies of shell mechanics and colloidal design, to the delivery of drugs, cosmetics, and industrial chemicals. An important direction for future work will be extending the range of stimuli that can trigger the microcapsule release, as well as designing microcapsules that respond to these stimuli in a variety of ways.

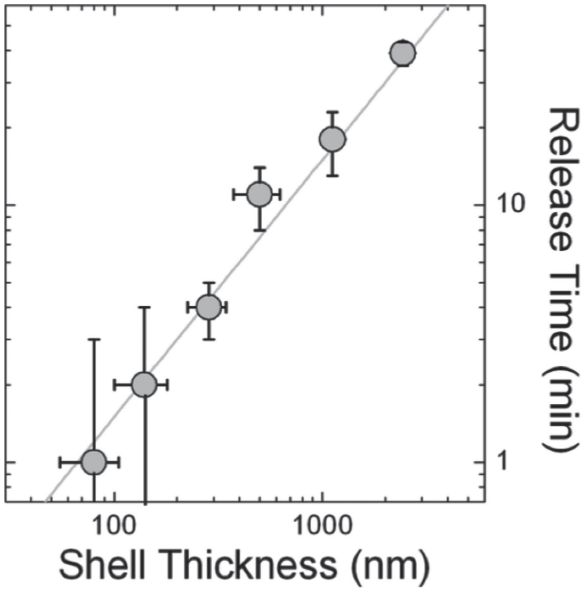

Figure 14. Time delay before release begins, quantified using fluorescence microscopy of double emulsion-templated pH-responsive microcapsules encapsulating a fluorescent dye, increases with increasing shell thickness. Vertical error bars show standard deviation in measured release time, while horizontal error bars show standard deviation in shell thickness of each batch. Reproduced with permission.[85] Copyright 2013, American Chemical Society.

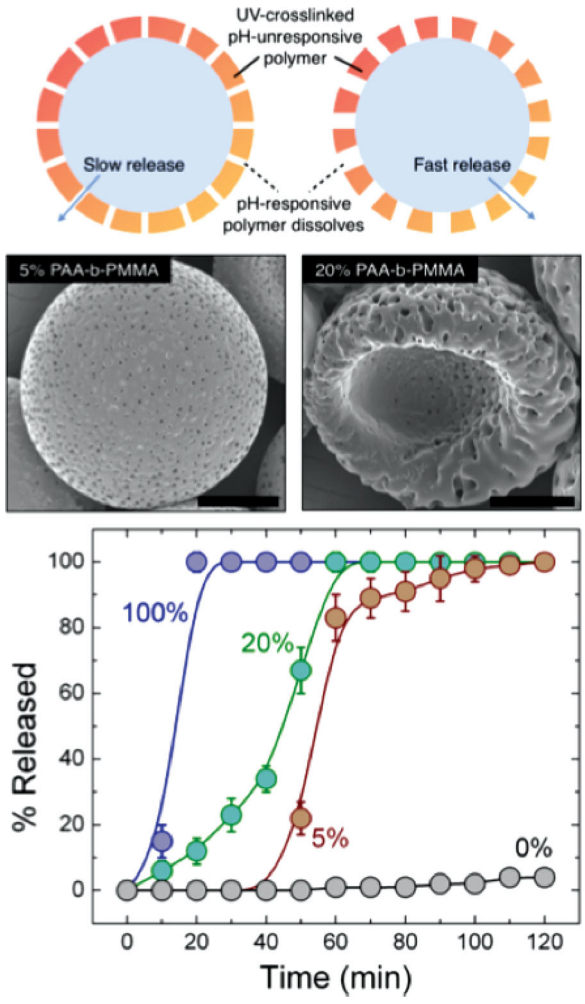

Figure 15. (Top) Schematic representation and (middle) scanning electron microscope micrographs of double emulsion-templated hybrid microcapsules with holes formed in their shells after degradation, triggered by exposure to an unfavorable pH. The size of the holes increases with increasing pH-responsive PAA-b-PMMA polymer content in the shell. Scale bars denote 80 μm. (Bottom) Amount of encapsulated material released, quantified by monitoring the relative intensity in the core of microcapsules encapsulating a fluorescent dye, increases with time; capsules are triggered at a basic pH. The rate at which the material is released increases with the PAA-b-PMMA content of the shell (percentage next to each curve). Vertical error bars show standard deviation of measured intensity in each batch, at each time point. Reproduced with permission.[85] Copyright 2013, American Chemical Society.

One limitation of the fabrication techniques described in this review is that they can typically only produce microcapsules of sizes on the order of tens or hundreds of micrometers. Many applications require even smaller microcapsules. Producing these, however, remains a challenge. It requires the use of capillaries with small orifices; forcing fluids through such

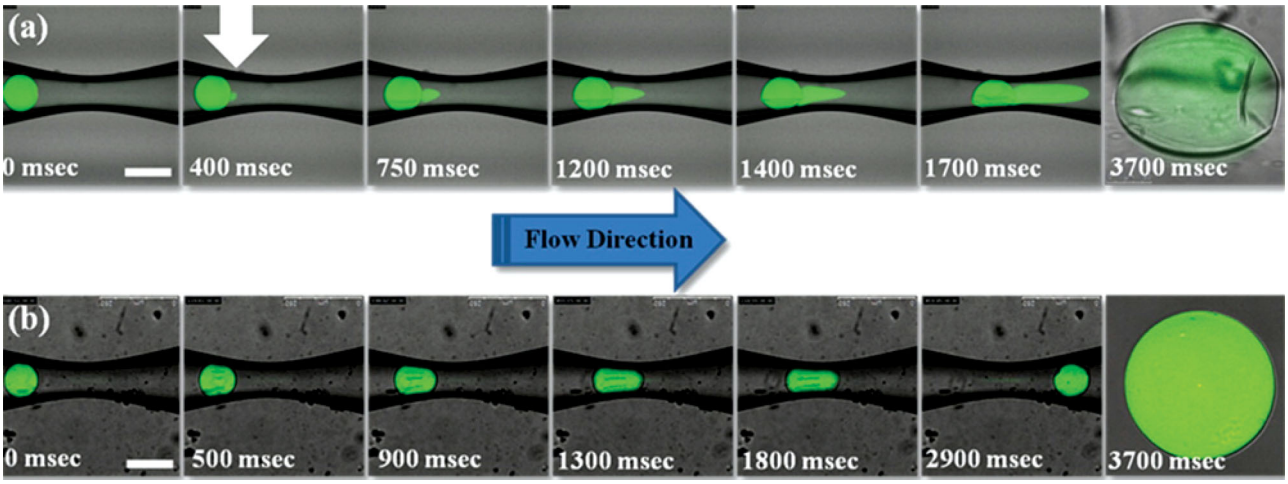

Figure 16. Confocal micrographs show (a) PS and (b) ductile PS-PIP-PS microcapsules being forced through a 70 μm diameter capillary constriction. The brittle PS shell ruptures, and the microcapsule releases its contents, while the ductile PS-PIP-PS remains intact and recovers its spherical shape. Scale bars denote 130 μm. Reproduced with permission.[84] Copyright 2013, American Chemical Society.

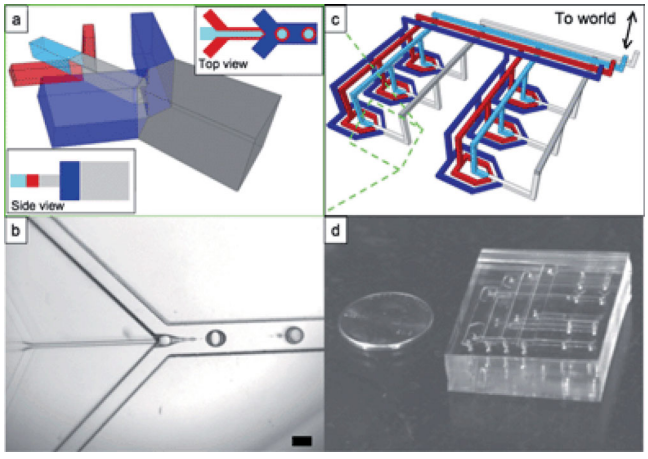

Figure 17. High-throughput production of double emulsion templates using a parallelized microfluidic chip. A single double emulsifier unit is shown schematically in (a) and using an optical micrograph in (b); scale bar denotes 100 μm. These are then parallelized, with rows of double emulsifier units connected through vertical through-holes to a layer of larger distribuion/collection channels, as shown schematically in (c) and using the photograph in (d). Each integrated row is connected to yet another layer of larger distribution/collection channels. The coin (a US penny) in (d) is 19 mm across. Reproduced with permission.[90] Copyright 2012, Royal Society of Chemistry.

narrow spaces results in prohibitively large pressures, whereas circumventing this requires the use of extremely small flow rates, which can be difficult to controllably achieve. Another important direction for future work will be to optimize the kinetics of microcapsule release: as exemplified by the data in Figures 7 and 9, the microcapsule release kinetics are often highly variable. This presumably reflects heterogeneities in the microcapsule shell structure or composition that arise during fabrication.

Many applications require the rapid production of large quantities of microcapsules. The double emulsions templates we use are produced drop by drop in a single glass capillary microfluidic device; this limits the rate at which they are produced, and hence, the rate at which microcapsules can be produced. However, it is possible to design microfluidic chips that operate many such devices in parallel; for example, we have shown that four glass capillary devices, similar to those described in this review, can be stably operated in parallel, enabling the production of double emulsion templates at a higher throughput.[89] We have also used soft lithography to incorporate up to 15 dropmaker units, arranged in both two- and three-dimensional arrays, in a polydimethylsiloxane (PDMS) device,[90] as shown in **Figure 17**. These chips can be used to produce highly monodisperse double emulsion templates at rates exceeding 1 kg day^{-1}, sufficient for many commercial situations. We expect that extensions of this work, integrating even more drop makers, will provide a route to industrial-scale production rates.

Acknowledgements

This article is part of an ongoing series celebrating the 25th anniversary of *Advanced Materials*. This work was supported by the NSF (DMR-1310266), the Harvard MRSEC (DMR-0820484), and the Advanced Energy Consortium (http://www.beg.utexas.edu/aec/), whose member companies include BP America Inc., BG Group, Petrobras, Schlumberger, Shell, and Total. SSD acknowledges support from ConocoPhillips. It is a pleasure to thank L. A. Arriaga for helpful comments on the manuscript. S.S.D. and A.A. contributed equally to this work.

Received: October 15, 2013
Revised: January 2, 2014
Published online:

[1] J. Sheng, Modern Chemical Enhanced Oil Recovery: Theory and Practice, Gulf Professional Publishing, **2010**.
[2] S. P. Friedman, Y. Mualem, *Fert. Res.* **1994**, *39*, 19.
[3] K. Tsuji, *J. Microencapsule* **2001**, *18*, 137.
[4] K. Hirech, S. Payan, G. Carnelle, L. Brujes, J. Legrand, *Powder Technol.* **2003**, *130*, 324.

DOI: 10.1002/adma.201305119

[5] C. C. Dowler, O. D. Dailey, B. G. Mullinix, J. Agric, *Food Chem.* **1999**, *47*, 2908.
[6] T. Takei, M. Yoshida, K. Yanagi, Y. Hatate, K. Shiomori, S. Kiyoyama, *Polymer Bulletin* **2008**, *61*, 119.
[7] S. Riyajan, J. T. Sakdapipanich, *Polymer Bulletin* **2009**, *63*, 609.
[8] O. D. Dailey, C. C. Dowler, B. G. Mullinix, J. Agric, *Food Chem.* **2003**, *41*, 1517.
[9] M. A. Augustin, Y. Hemar, *Chem. Soc. Rev.* **2009**, *38*, 902.
[10] A. Madene, M. Jacquot, J. Scher, S. Desobry, *Int. J. Food Sci. Technol.* **2006**, *41*, 1.
[11] D. J. McClements, E. A. Decker, J. Weiss, *J. Food Sci.* **2007**, *72*, 109.
[12] R. Wegmuller, M. B. Zimmermann, V. G. Buhe, E. J. Windhab, R. F. Hurrell, *J. Food Sci.* **2006**, *71*, 2.
[13] B. G. De Geest, C. De Jugnat, E. Verhoeven, G. B. Sukhorukov, A. M. Jonas, J. Plain, J. Demeester, S. C. De Smedt, *J. Controlled Release* **2006**, *116*, 159.
[14] G. Ibarz, L. Dahne, E. Donath, H. Mohwald, *Adv. Mat.* **2001**, *13*, 1324.
[15] S. Ye, C. Wang, X. Liu, Z. Tong, B. Ren, F. Zeng, *J. Controlled Release* **2006**, *112*, 79.
[16] H. Ai, S. A. Jones, M. M. Villiers, Y. M. Lvov, *J. Controlled Release* **2003**, *86*, 59.
[17] S. H. Hu, C. H. Tsai, C. F. Liao, D. M. Liu, S. Y. Chen, *Langmuir* **2008**, *24*, 11811.
[18] D. G. Shchukin, D. A. Gorin, H. Mohwald, *Langmuir* **2006**, *22*, 7400.
[19] B. G. De Geest, A. G. Skirtach, A. A. Mamedov, A. A. Antipov, N. A. Kotov, S. C. De Smedt, G. B. Sukhorukov, *Small* **2007**, *3*, 804.
[20] C. H. Choi, J. H. Jung, D. W. Kim, Y. M. Chung, C. S. Lee, *Lab Chip* **2008**, *8*, 1544.
[21] T. He, K. Zhang, X. Mu, T. Luo, Y. Wang, G. Luo, *Microfluid. Nanofluid.* **2011**, *10*, 1289.
[22] R. Karnik, F. Gu, P. Basto, C. Cannizzaro, L. Dean, W. Kyeimanu, R. Langer, O. C. Farokhzad, *Nano Lett.* **2008**, *8*, 2906.
[23] K. Saskia, L. Peter, S. Ute, N. Hiroshi, *Fragrance Journal* **2005**, *33*, 51.
[24] K. Miyazawa, I. Yajima, I. Kaneda, T. Yanaki, *J. Cosmet. Sci.* **2000**, *51*, 239.
[25] M. Jacquemond, N. Jeckelmann, L. Ouali, O. P. Haefliger, *Journal of Applied Polymer Science* **2009**, *114*, 3074.
[26] T. Feczko, V. Kokol, B. Voncina, *Macromolecular Research* **2010**, *18*, 636.
[27] R. Badulescu, V. Vivod, D. Jausovec, B. Voncina, *Carbohyd. Polym.* **2008**, *71*, 85.
[28] G. Orive, R. M. Hernandez, A. R. Gascon, R. Calafiore, T. M. S. Chang, P. de Vos, G. Hortelano, D. Hunkeler, I. Lacik, A. M. Shapiro, J. L. Pedraz, *Nat. Med.* **2003**, *9*, 104.
[29] N. C. Hunt, L. M. Grover, *Biotechnol. Lett.* **2010**, *32*, 733.
[30] T. Joki, M. Machluf, A. Atala, J. Zhu, N. T. Seyfried, I. F. Dunn, T. Abe, R. S. Carroll, *Nat. Biotechnol.* **2001**, *19*, 35.
[31] T. M. S. Chang, *Nat. Rev. Drug Discov.* **2005**, *4*, 221.
[32] T. Vermonden, N. E. Fedorovich, D. van Geemen, J. Alblas, C. F. van Nostrum, W. J. A. Dhert, W. E. Hennink, *Biomacromolecules* **2008**, *9*, 919.
[33] H. Uludag, P. de Vos, P. A. Tresco, *Adv. Drug Deliv. Rev.* **2000**, *42*, 29.
[34] W. Qi, X. Yan, L. Duan, Y. Cui, Y. Yang, J. Li, *Biomacromolecules* **2009**, *10*, 1212.
[35] M. J. McShane, J. Q. Brown, K. B. Guice, Y. M. Lvov, *Nanoscience and Nan-otechnology* **2002**, *2*, 411.
[36] L. I. Kazakova, L. I. Shabarchina, G. B. Sukhorukov, *Phys. Chem. Chem. Phys.13*, 11110, **2011**.
[37] L. E. Sinks, G. P. Robbins, E. Roussakis, T. Troxler, D. A. Hammer, S. A. Vino-gradov, *J. Phys. Chem. B* **2010**, *114*, 14373.
[38] S. L. Poe, M. Kobaslija, D. T. McQuade, *J. Am. Chem. Soc.* **2007**, *129*, 9216.
[39] C. Ramaraoa, S. V. Ley, S. C. Smith, I. M. Shirley, N. DeAlmeidac, *Chem. Commun.* **2002**, *13*, 1132.
[40] B. J. Blaiszik, M. M. Caruso, D. A. McIlroy, J. S. Moore, S. R. White, N. R. Sottos, *Polymer* **2009**, *50*, 990.
[41] E. N. Brown, S. R. White, N. R. Sottos, *Journal of Materials Science* **2004**, *39*, 1703.
[42] M. A. White, *J. Chem. Educ.* **1998**, *75*, 1119.
[43] B. Comiskey, J. D. Albert, H. Yoshizawa, J. Jacobson, *Nature* **1998**, *394*, 253.
[44] C. A. Kim, M. J. Joung, S. D. Ahn, G. H. Kim, S. Y. Kang, I. K. You, J. Oh, H. J. Myoung, K. H. Baek, K. S. Suh, *Synthetic Metals* **2005**, *151*, 181.
[45] Y. Chen, J. Au, P. Kazlas, A. Ritenour, H. Gates, M. McCreary, *Nature* **2003**, *136*, 423.
[46] Y. K. Hwang, U. Jeong, E. C. Cho, *Langmuir* **2008**, *24*, 2446.
[47] C. J. Park, Y. K. Hwang, D. C. Hyun, U. Jeong, *Macromol. Rapid Commun.* **2010**, *31*, 1713.
[48] L. B. Petrovic, V. J. Sovilj, J. M. Katona, J. L. Milanovic, *J. Colloid Interface Sci.* **2010**, *342*, 333.
[49] R. Bocanegra, A. G. Gaonkar, A. Barrero, I. G. Loscertales, D. Pechack, M. Mar-quez, *Journal of Food Science* **2005**, *70*, 8.
[50] H. Chen, Y. Zhao, Y. Song, L. Jiang, *J. Am. Chem. Soc.* **2008**, *130*, 7800.
[51] Y. Fukui, T. Maruyama, Y. Iwamatsu, A. Fujii, T. Tanaka, Y. Ohmukai, H. Mat-suyama, *Colloids and Surfaces A* **2010**, *370*, 28.
[52] F. V. Lamberti, R. A. Evangelista, J. Blysniuk, M. A. Wheatley, M. V. Sefton, *Microencapsulation and Artificial Cells* **1985**, *7*, 101.
[53] J. R. Hwang, M. V. Sefton, *Journal of Controlled Release* **1997**, *49*, 217.
[54] Q. Wen-tao, Y. Wei-ting, X. Yu-bing, M. Xiaojun, *Biochemical Engineering Jour-nal* **2005**, *25*, 151.
[55] K. Bouchemal, S. Briancon, E. Perrier, H. Fessi, I. Bonnet, N. Zydowicz, *Int. J. Pharm* **2004**, *269*, 89.
[56] T. Dobashi, F. J. Yeh, Q. C. Ying, K. Ichikawa, B. Chu, *Langmuir* **1995**, *11*, 4278.
[57] T. Dobashi, T. Furukawa, T. Narita, S. Shimofure, K. Ichikawa, B. Chu, *Langmuir* **2001**, *17*, 4525.
[58] A. Loxley, B. Vincent, *J. Colloid Interface Sci.* **1998**, *208*, 49.
[59] P. J. Dowding, R. Atkin, B. Vincent, P. Bouillot, *J. Am. Chem. Soc.* **2004**, *20*, 11374.
[60] M. J. McShane, J. Q. Brown, K. B. Guice, Y. M. Lvov, *J. Nanosci. Nanotechnol.* **2002**, *2*, 411.
[61] N. G. Balabushevich, O. P. Tiourina, D. V. Volodkin, N. I. Larionova, G. B. Sukhorukov, *Biomacromolecules* **2003**, *4*, 1191.
[62] D. Shchukin, T. Shutava, G. Sukhorukov, Y. M. Lvov, *Chem. Mater.* **2004**, *16*, 3446.
[63] K. Akamatsu, W. Chen, Y. Suzuki, T. Ito, A. Nakao, T. Sugawara, R. Kikuchi, S. Nakao, *Langmuir* **2010**, *26*, 14854.
[64] Q. Yuan, R. A. Williams, S. Biggs, *Colloids Surf. A* **2009**, *347*, 97.
[65] A. S. Utada, E. Lorenceau, D. R. Link, P. D. Kaplan, H. A. Stone, D. A. Weitz, *Science* **2005**, *308*, 537.
[66] G. T. Vladisavljevic, H. C. Shum, D. A. Weitz, *Progr. Colloid Polym. Sci.* **2012**, *139*, 115.
[67] S. S. Datta, S. H. Kim, J. Paulose, A. Abbaspourrad, D. R. Nelson, D. A. Weitz, *Phys. Rev. Lett.* **2012**, *109*, 134302.
[68] L. S. Mok, K. Kim, *J. Fluid Mech.* **1987**, *176*, 521.
[69] S. H. Kim, J. W. Kim, J. C. Cho, D. A. Weitz, *Lab on a Chip* **2011**, *11*, 3162.
[70] L. L. A. Adams, T. E. Kodger, S. H. Kim, H. C. Shum, T. Franke, D. A. Weitz, *Soft Matter* **2012**, *8*, 10719.
[71] S. H. Kim, S. J. Jeon, S. M. Yang, *J. Am. Chem. Soc.* **2008**, *130*, 6040.
[72] R. C. Hayward, A. S. Utada, N. Dan, D. A. Weitz, *Langmuir* **2006**, *22*, 4457.
[73] L. D. Landau, E. M. Lifshitz, *Theory of Elasticity*, 3rd ed. Elsevier, New York **1986**.
[74] A. Fery, F. Dubreuil, H. Mohwald, *New J. Phys.* **2004**, *6*, 18.

[75] A. Abbaspourrad, W. J. Duncanson, N. Lebedeva, S.-H. Kim, A. Zhushma, S. S. Datta, S. S. Sheiko, M. Rubinstein, D. A. Weitz, *Langmuir* **2013**, *29*, 12352.
[76] N. Vilanova, C. Rodríguez-Abreu, A. Fernández-Nieves, C. Solans, *ACS Appl. Mat. Int.* **2013**, *5*, 5247.
[77] J. Paulose, D. R. Nelson, *Soft Matter* **2013**, *9*, 8227.
[78] S. Sacanna, W. T. Irvine, P. M. Chaikin, D. J. Pine, *Nature* **2010**, *464*, 575.
[79] B. J. Sun, H. C. Shum, C. Holtze, D. A. Weitz, *ACS Applied Materials and Interfaces* **2010**, *2*, 3411.
[80] M. Windbergs, Y. Zhao, J. Heyman, D. A. Weitz, *J. Am. Chem. Soc.* **2013**, *135*, 7933.
[81] A. Fernandez-Nieves, H. Wyss, J. Mattson, D. A. Weitz, Microgel Suspensions: Fundamentals and Applications, Wiley-VCH, **2011**.
[82] E. Amstad, S. H. Kim, D. Weitz, *Angew. Chem. Int. Ed.* **2012**, *51*, 12499.
[83] S. Zhou, J. Fan, S. S. Datta, M. Guo, X. Guo, D. A. Weitz, *Adv. Func. Mater.* **2013**, *23*, 5925.
[84] A. Abbaspourrad, N. J. Carroll, S. H. Kim, D. A. Weitz, *J. Am. Chem. Soc.* **2013**, *135*, 7744.
[85] A. Abbaspourrad, S. S. Datta, D. A. Weitz, *Langmuir* **2013**, *29*, 12697.
[86] A. S. Miguel, J. Scrimgeour, J. E. Curtis, S. H. Behrens, *Soft Matter* **2010**, *6*, 3163.
[87] S. S. Datta, A. Abbaspourrad, D. A. Weitz, *Materials Horizons* **2013**, *1*, 92.
[88] A. M. DiLauro, A. Abbaspourrad, D. A. Weitz, S. T. Phillips, *Macromolecules* **2013**, *46*, 3309.
[89] S. H. Kim, J. W. Kim, D. H. Kim, S. H. Han, D. A. Weitz, *Microfluid. Nanofluid.* **2013**, *14*, 509.
[90] M. B. Romanowsky, A. R. Abate, A. Rotem, C. Holtze, D. A. Weitz, *Lab on a Chip* **2012**, *12*, 802.

Adv. Mater. **2014**,
DOI: 10.1002/adma.201305119